Pergamon

PII: S0306-4522(01)00261-5

www.elsevier.com/locate/neuroscience

Neuroscience Vol. 106, No. 2, pp. 419–432, 2001

0306-4522/01 $20.00+0.00

ALTERNATE SPLICING OF THE *SHAL* GENE AND THE ORIGIN OF I_A DIVERSITY AMONG NEURONS IN A DYNAMIC MOTOR NETWORK

D. J. BARO,[a,b]* L. QUIÑONES,[a] C. C. LANNING,[b] R. M. HARRIS-WARRICK[b] and M. RUIZ[a]

[a]Institute of Neurobiology and Department of Biochemistry-Medical Sciences Campus, University of Puerto Rico, San Juan, PR, USA

[b]Department of Neurobiology and Behavior, Cornell University, Ithaca, NY, USA

Abstract—The pyloric motor system, in the crustacean stomatogastric ganglion, produces a continuously adaptive behavior. Each cell type in the neural circuit possesses a distinct yet dynamic electrical phenotype that is essential for normal network function. We previously demonstrated that the transient potassium current (I_A) in the different component neurons is unique and modulatable, despite the fact that the *shal* gene encodes the α-subunits that mediate I_A in every cell. We now examine the hypothesis that alternate splicing of *shal* is responsible for pyloric I_A diversity. We found that alternate splicing generates at least 14 isoforms. Nine of the isoforms were expressed in *Xenopus* oocytes and each produced a transient potassium current with highly variable properties. While the voltage dependence and inactivation kinetics of I_A vary significantly between pyloric cell types, there are few significant differences between different shal isoforms expressed in oocytes. Pyloric I_A diversity cannot be reproduced in oocytes by any combination of shal splice variants.

While the function of alternate splicing of *shal* is not yet understood, our studies show that it does not by itself explain the biophysical diversity of I_A seen in pyloric neurons.

Key words: Kv, stomatogastric, alternate splicing, gene expression, potassium channel, A-current.

Dynamic neural networks face a difficult organizational problem: the neurons must be capable of significant modulation in their firing properties, yet each neuron must have its own identity with a distinct set of intrinsic firing properties. In relatively stable systems, different baseline properties in the component cells arise from fixed differences in the expression of ion channel α-subunits. In the cochlea, for example, the number and type of 'BK' calcium-activated K^+ channels vary methodically along the tonotopic axis. BK α-subunits with different kinetics are created by alternate splicing of the *slo* gene, and different slo isoforms are expressed according to the hair cell's position along the tonotopic axis (Navaratnam et al., 1997; Rosenblatt et al., 1997; Jones et al., 1999a,b). Apical to basilar positional differences in *slo* expression levels and isoform expression patterns contribute to a systematic variation in the kinetic properties of the BK current along the axis that corresponds to the axial variation in the frequency response characteristics of the hair cells (Fettiplace and Fuchs, 1999; Oberholtzer, 1999; Ramanathan et al., 1999). Are fixed differences in ion channel α-subunit gene expression also used to establish differences in the properties of neurons in rapidly adapting systems, or do fundamental molecular organizing principles differ between dynamic and stable networks?

In the spiny lobster, *Panulirus interruptus*, the continuously adaptive pyloric network contains 14 neurons that fall into six cell types. Each pyloric cell type possesses a unique, modulatable transient potassium current, or A-current (I_A), that is instrumental in determining the ever-changing output of this network (Hartline, 1979; Graubard and Hartline, 1991; Tierney and Harris-Warrick, 1992; Harris-Warrick et al., 1995a,b; Baro et al., 1997). The baseline differences between the six pyloric I_As are well defined and include differences in amplitude, voltage dependence, and kinetics. Surprisingly, we discovered that although the I_A is distinct in every cell type, the *shal* gene encodes the A-channel α-subunits in the somatodendritic compartment of all pyloric neurons (Baro et al., 1997, 2000). Quantitative differences in the level of shal gene expression account for differences in A-channel density between cells, but they cannot account for differences in the voltage dependence or kinetics of the various pyloric I_As. In this paper we examined the hypothesis that cell-specific alternate

*Correspondence to: D.J. Baro, Institute of Neurobiology, 201 Boulevard del Valle, San Juan, PR 00901, USA. Tel.: +1-787-724-2364; fax: +1-787-725-3804.

E-mail address: djbaro@neurobio.upr.clu.edu (D. J. Baro).

Abbreviations: AB, anterior burster; I_A, transient potassium current or A-current; IC, inferior cardiac; LP, lateral pyloric; PCR, polymerase chain reaction; PD, pyloric dilator; (p)ORF, (partial) open reading frame; PY, pyloric constrictor; RACE, rapid amplification of cDNA ends; RT, reverse transcription; UAP, universal amplification primer; UTR, untranslated region; V_{act}, voltage of half activation; VD, ventricular dilator; V_{inact}, voltage of half inactivation.

splicing of the *shal* transcript is responsible for pyloric I_A diversity.

EXPERIMENTAL PROCEDURES

Isolating alternate splice forms with modified 3′ rapid amplification of cDNA ends (RACE) techniques

We used two different methods to isolate alternate splice forms of lobster *shal*. Both methods are modifications of 3′ RACE (Frohman, 1990), and both methods use a set of three lobster *shal*-specific oligonucleotides (Cornell Biotechnology Facility, Ithaca, NY, USA). The oligonucleotide sets used in the various reactions are listed in Table 1-REF>, and their positions are shown in Fig. 1. mRNA was isolated from the brain and ventral nerve cord and reverse transcribed as previously described (Baro et al., 1994). In the first method, randomly primed first strand cDNA was amplified in a nested polymerase chain reaction (PCR) using either an OmnE (Hybaid, Ashford, Middlesex, UK) or 480 (Perkin Elmer, Indianapolis, IN, USA) thermal cycler, and reaction conditions that varied with the primer sets according to standard principles (Innis et al., 1990, 1995). The 5′ primer in the first PCR is specific for the *shal* gene. The 3′ primer contains a random 15-mer at its 3′ end and a universal amplification primer (UAP) site at its 5′ end. UAP is simply a convenient sequence of 30 nucleotides. In the first cycle of the first PCR, the *shal*-specific primer will bind the minus strand of the cDNA and be extended in the carboxy-terminal direction. The annealing is carried out at high stringency where the *shal*-specific primer can bind efficiently, but the random 15-mer UAP primer cannot. Thus, during this cycle, *shal* plus strands are preferentially synthesized. This cycle is repeated a few times to create a greater pool of *shal* plus strands. In the next few cycles, the annealing temperature is reduced. This allows the random 15-mer portion of the 3′ primer to bind to homologous regions of the newly made *shal* plus strands. The bound primers are then extended toward the amino-terminus. After a few cycles at the reduced annealing temperature, we once again raise the annealing temperature. The random 15-mer portion of the 3′ primer can no longer bind efficiently at this temperature. However the *shal*-specific primer and the entire 3′ primer (15-mer+UAP) bind well to regions of perfect homology. Thus during subsequent cycles we amplify the existing products rather than create new products. Next, we perform a nested PCR to selectively amplify the *shal*-specific products of the first PCR over background products. This is a standard PCR in which the second 5′ primer is immediately downstream of the first, and the 3′ primer is UAP. A Southern blot analysis is performed on the nested PCR product, and the probe is a third *shal*-specific oligonucleotide, located downstream of the second 5′ primer. Lastly, we cloned and sequenced the bands that gave a positive signal on the Southern blot. Gel electrophoresis and Southern blotting were performed as previously described (Baro et al., 1994). The major drawback to this method is the creation of false positives in which the 15-mer binds the minus strand of the DNA in the first few cycles of the PCR, so that we end up with products containing the 15-mer UAP at both ends and no *shal* primer. To reduce the number of false positives, we reduce the concentration of the 15-mer UAP primer 50-fold, relative to the *shal*-specific primer. We also reduce the cycle number in the first PCR (15–20 cycles). The bulk of the amplification occurs in the second PCR (35 cycles).

In the second method, we used a Marathon kit (Clonetech, Palo Alto, CA, USA). This kit uses a similar strategy to that described above. The major difference is that the 3′ primer in the Marathon kit has been engineered to prevent the formation of false positives. Once we had tailored the Marathon procedure to isolate lobster *shal* transcripts using the guidelines provided with the kit, the method worked extremely well in our hands and the number of false positives obtained was significantly reduced. In either method, resulting bands were isolated from acrylamide or agarose gels using standard procedures (Ausubel et al., 1990), and cloned into a dephosphorylated, blunt-ended Bluescript vector as previously described (Baro et al., 1994). The Cornell Biotechnology Sequencing Facility performed sequencing. For every splice form, we isolated at least two independent clones from different RACE/Marathon reactions. In many instances the same carboxy-end was isolated with both methods.

Constructing full-length clones

Standard restriction digests and ligations (Ausubel et al., 1990) were used to produce full-length constructs in a Bluescript vector. Constructs were transformed into subcloning grade XL1-Blue cells (Stratagene, La Jolla, CA, USA) and glycerol stocks were maintained at −70°C.

Oocyte injections and electrophysiology

Oocytes were harvested and maintained as previously described (Baro et al., 1996). RNA was transcribed and capped using a T3 mMessage mMachine kit (Ambion, Austin, TX, USA). The transcripts were digested with DNase, phenol/$CHCl_3$ extracted, precipitated and resuspended in sterile distilled H_2O. 100 nl of a 0.1 to 1 μg/ml solution was injected with a sterile glass microelectrode using a microinjector (Sutter Instruments, Novato, CA, USA). Various amounts of RNA were injected in order to determine optimal expression. The only factor that appeared to vary with the amount of RNA injected was the current amplitude. A two-microelectrode voltage clamp (Axoclamp2B or Geneclamp, Axon Instruments, Foster City, CA, USA) was used to record currents 2–5 days after injection. Microelectrodes were filled with 3 M KCl and had a tip resistance ≤ 1 MΩ. All recordings were at 16 ± 1°C using previously described solutions (Baro et al., 1996). Oocytes were held at −50 mV. To measure inactivation kinetics, a 1-s hyperpolarizing prepulse to −90 mV was followed by a depolarizing test pulse to +20 mV for 1 to 4 s. The voltage dependence of activation was determined by varying the test pulse from −70 mV to +40 mV in 10-mV increments. The steady-state inactivation was determined by varying a 10-s hyperpolarizing prepulse from −100 mV to −40 mV in 8-mV increments. To remove the contribution of endogenous currents expressed by the oocyte, 3–5 H_2O-injected oocytes were recorded each day. The resulting control traces were averaged and the appropriate control trace was digitally subtracted from each experimental shal trace recorded on the same day, before the shal trace was analyzed as described below. The oocyte currents usually ranged from 50 to 100 nA. All currents were leak-subtracted on-line using a P/4 procedure, and low-pass filtered at 500 Hz using a Bessel Filter (Frequency Devices, Havaerhill, MA, USA).

Data acquisition and analysis

Voltage clamp protocols and data acquisition were controlled by a 486 PC desktop computer (Gateway) interfaced to a 12-bit A/D converter (Digidata 1200, Axon Instruments) using pClamp 6 (Axon Instruments).

Kinetic analysis. The Clampfit program in pClamp 8 (Axon Instruments) was used to analyze the inactivation kinetics. Every trace was analyzed with two fitting algorithms: Chebyshev and Simplex. The data for a given trace were used only if the results of the two procedures agreed. Current decay was described with the following exponential equation:

$$I(t) = A_0 \exp(-t/\tau_0) + \ldots + A_n \exp(-t/\tau_n) + C,$$

where A_0 and A_n are the amplitudes of the exponential terms and τ_0 and τ_n are the corresponding time constants. C is a constant that represents the steady-state level of the current. Every trace was fit with a first, second, and third order equation. A given exponential equation was deemed appropriate when it produced a good visual fit (there were no obvious gaps between the line and the trace), and a higher order equation did not

significantly improve the fit (r^2 increased by <0.01). In our fitting protocol, the first cursor was placed just after the peak and the second cursor was placed at the end of the trace, 5–10 ms before the end of the test pulse. After fitting the trace and defining the correct number of exponentials, the first cursor was moved to the right by roughly 30 ms and the trace was refit with Chebyshev and Simplex algorithms in order to demonstrate that the results did not change significantly. In order to show that the difference in the fitting protocol was not responsible for the difference between shal currents expressed in oocytes and pyloric neurons, we refit all Type I shal currents expressed in oocytes by placing the second cursor midway through the 1-s test pulse. Depending upon the isoform, 25–75% of the currents could not be fit to this shorter step. Of those that could be fit, the time constants changed on average by 10% in either direction, and τ_2 of only five oocytes overlapped with that of pyloric neurons. Thus, the differences in the fitting protocols could not account for the large differences observed between shal expression in pyloric cells and oocytes.

Analysis of voltage dependence. The Clampfit program of pClamp 6 (Axon Instruments) and Deltagraph 4.5 (SPSS, Richmond, CA, USA) were used to analyze the voltage dependence of activation and inactivation as previously described (Baro et al., 1996). The g/V curves were fit to a third (activation) or first (inactivation) order Boltzmann equation of the form:

$$g = g_{max}[1/(1 + e^{-(V-V_{act}/s)})]^n$$

where g_{max} is the maximal conductance, s is the slope factor, V_{act} is the voltage of half maximal activation for individual gating steps, and n is 3 (activation) or 1 (inactivation). The peak conductance of a window current was defined as the conductance at the peak voltage and calculated as the product of the activation curve cubed (m^3) and the inactivation curve (h) at that voltage.

Statistical analysis. An analysis of variance was performed to determine significant differences between isoforms unless otherwise indicated. The Games/Howell procedure was used as the post hoc test; though relatively conservative, it does not assume homogeneity of variance, equal numbers between categories, or normality within a category. All statistical analyses were performed with StatView (SAS) and Excel (Microsoft). In all instances $P<0.05$, was considered statistically significant.

RESULTS

Obtaining alternately spliced shal transcripts

Our previous studies suggested that alternate splicing does not occur at the 5′ end of the lobster *shal* open reading frame (ORF). Twenty independently isolated, overlapping *shal* clones from several cDNA libraries and reverse transcription (RT)-PCRs were identical over the segment beginning in the 5′ untranslated region (UTR) and extending beyond the traditionally defined conserved core of the Shaker family of voltage dependent K^+ channels (Wei et al., 1990; Baro et al., 1994, 1996). In addition, we found that the lobster *shal* gene did not contain introns in the region bounded by the cloned portion of the UTR and the first membrane-spanning region (Baro et al., 1996). However, we did find evidence for introns 3′ to the sixth membrane-spanning region. This region is not well conserved across species, and alternate splicing of *Drosophila* and mammalian *shal* transcripts occurs in this region (Wei et al., 1990; Isbrandt et al., 2000). Because screening more than 10^6 clones from each of four different cDNA libraries yielded only one clone containing the carboxy-terminus of the lobster *shal* ORF, we searched for alternate splicing at the 3′ end of the *shal* transcript using two different techniques, both of which were modifications on 3′ RACE, as described in Experimental procedures.

In these experiments, lobster *shal*-specific oligonucleotides (primers) from an invariant region of the protein were hybridized to first strand cDNA that represented a population of lobster transcripts isolated from the nervous system (Table 1, Fig. 1). The primers bound to *shal* transcripts and were extended in the 3′ direction. The extended primers were then amplified, cloned, and sequenced as described in Experimental procedures. We obtained multiple sequences that were identical at the 5′ end but then diverged at the same point, indicative of alternate splicing at the carboxy-terminus of lobster *shal* transcripts. To extend the alternate splice forms that did not contain stop codons, and to search for additional points of alternate splicing, we repeated our experiments using additional primer sets downstream of the original primers (Table 1). These experiments yielded six alternately spliced *shal* transcripts: shal 1.a through shal 1.f. The complete shal transcript is illustrated in Fig. 1 as a collection of partial ORF (pORF), where a pORF corresponds to one or more exons. Each of the six alternately spliced transcripts is listed below the diagram, and the different combination of pORFs in each transcript is indicated.

We next asked if adding or deleting pORFs from the six original transcripts created additional transcripts. We designed 5′ and 3′ primers specific to the different pORFs, or unique UTRs, as shown in Fig. 1. Primers from two different pORFs (or UTRs) were used in PCRs with a randomly primed lobster nervous system cDNA template followed by Southern blot hybridization. The PCRs should produce various bands of predicted sizes on the gels and Southern blots, according to which primer sets were used. Bands of unexpected sizes indicate novel splice forms. Only two experiments yielded reproducible bands of unexpected sizes (Fig. 2). A nested PCR series with primer set (25:pORF P+44:pORF O) followed by (26:pORF P+44:pORF O) produced two

Table 1. Primer/probe sets

Reaction	First primer	Second primer	Probe for Southern blotting
Method 1; reactions 1 and 2	15	16	17
Method 2; reactions 1 and 2	25	26	27
Method 2; reaction 3	25	22	24
Method 2; reaction 4	15	36	–
Method 2; reaction 5	23	24	43

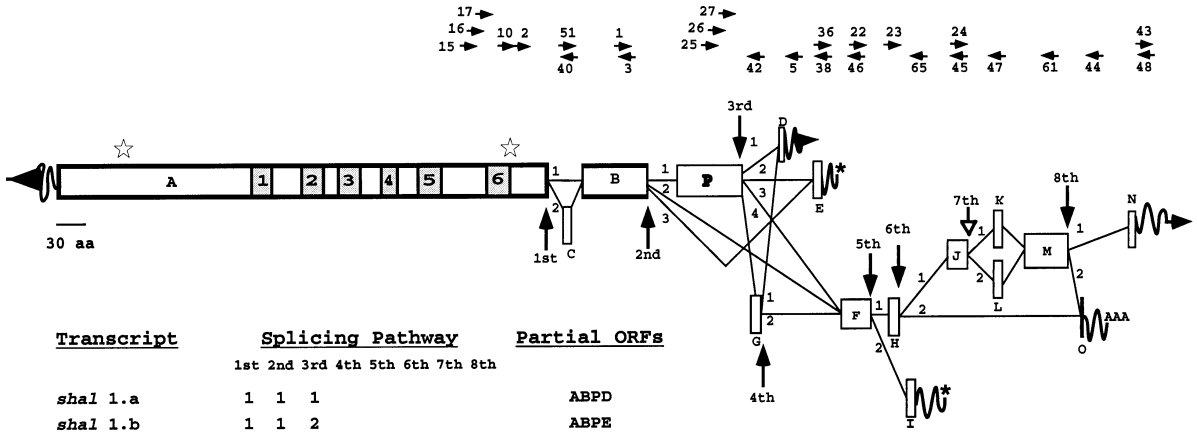

Transcript	Splicing Pathway								Partial ORFs
	1st	2nd	3rd	4th	5th	6th	7th	8th	
shal 1.a	1	1	1						ABPD
shal 1.b	1	1	2						ABPE
shal 1.c	2	1	2						ACBPE
shal 1.d	1	1	3	-	1	1	1	2	ABPFHJKMO
shal 1.e	1	1	3	-	1	1	2	2	ABPFHJLMO
shal 1.f	1	1	4	2	1	1	2	1	ABPGFHJLMN
shal 1.g	1	1	3	-	2				ABPFI
shal 1.h	1	1	3	-	1	2			ABPFHO
shal 1.i	1	2	-	-	1	1	2	2	ABFHJLMO
shal 1.j	2	1	4	2	?	?	?	?	ACBPGF..
shal 1.k	2	1	3	-	?	?	?	?	ACBPF...
shal 1.l	2	2	-	-	?	?	?	?	ACBF...
shal 1.m	2	3							ACBE
shal 1.n	1	1	4	1					ABPGD
shal 1.z	1	1	4	2	1	1	2	2	ABPGFHJLMO

Fig. 1. Alternate splicing of the lobster *shal* transcript. The diagram illustrates the various ways in which a *shal* transcript may be spliced. Each point of alternate splicing is indicated by a vertical arrow labeled 1st through 8th. The 16 boxes, labeled A–P, represent pORFs comprised of one or more exons. The pORFs are drawn to scale. The six membrane-spanning domains found in pORF A are shown as stippled boxes labeled 1–6. Stars above pORF A indicate the boundaries of the central conserved core region, which is highly conserved among all members of the Shaker family. The numbered lines between pORFs represent the possible paths at each alternate splice point. Wavy lines, which are not drawn to scale, represent 5′ and 3′ UTRs that either end in a poly A tract (AAA), continue for an undetermined number of nucleotides (arrows), or are spliced to what is a partial ORF in other transcripts (*). For example, the UTRs following pORFs E and I are spliced to pORFs F and O, respectively. Since there is a stop codon prior to F and O (at the end of pORFs E and I), F and O and are no longer ORFs in these transcripts, but are part of the UTR. The 15 transcripts described in the paper are listed (shal 1.a-shal 1.n. and shal 1.z). shal 1.z is an artificial construct; the corresponding transcript has not been found in the lobster nervous system. The paths taken at each of the eight alternate splice points is indicated for each transcript, as are the pORFs contained within the transcript. The arrows above the diagram represent the position of the oligonucleotides described throughout the text. The direction of the arrow indicates whether the oligonucleotide is extended in the amino- or carboxy-terminal direction. aa, amino acid.

bands on the gel and Southern blot [Fig. 2A, lanes 2 and 4)]. The higher 478-bp band is the correct size for a PCR product resulting from transcripts shal 1.d and/or shal 1.e, while the lower band was unexpected. Cloning and sequencing the products revealed that the upper band contained sequences corresponding to shal 1.e, and an unexpected, novel shal 1.g, while the lower band contained sequences corresponding to the new shal 1.h (see Fig. 1 legend). shal 1.i was cloned in a similar experiment shown in Fig. 2B. Nested PCRs with primer sets (17:pORF A+46:pORF F) (10:pORF A+46:pORF F) or (17:pORF A+45:pORF J) (10: pORF A+45:pORF J) consistently produced two bands of the expected sizes corresponding to shal splice forms 1.d-1.h, with the higher band representing transcripts that contained pORF G. In addition, these PCRs always produced a band that was 156 bp smaller than expected. Cloning and sequencing revealed that the new shal 1.i isoform was identical to shal 1.e, except that it lacked pORF P.

Some of the pORFs are very small and may not produce a detectable change in the size of the PCR product when added or deleted. Thus, we analyzed the products from the aforementioned PCRs with Southern blots using probes from small pORFs that were and were not expected to be in a specific PCR product. Fig. 2C illustrates this type of experiment. Up to this point, the 30-bp pORF C had only been found in the transcript shal 1.c (Fig. 1). We asked if pORF C could be associated with any of the other seven transcripts (1.a, 1.d–1.i). When an oligonucleotide from pORF C (40) was used to probe a Southern blot containing a PCR product amplified with primers 10:pORF A and 5:pORF D, and thus corresponding to transcript shal 1.a, no positive signal was produced (Fig. 2C, lanes 1 and 4). When primers 10:pORF A and 46:pORF F were used in the PCR, they produced three different size products (Fig. 2C, lane 2). The largest band corresponded to transcript shal 1.f. The middle band corresponded to transcripts 1.d, 1.e, 1.g, and 1.h. The lowest band corresponded to shal 1.i. All three bands produced a positive signal when probed with

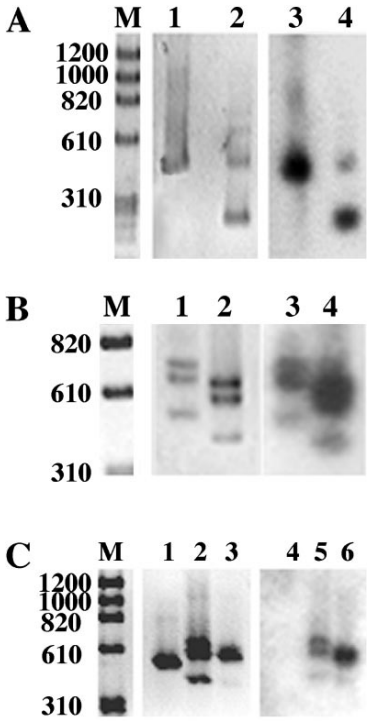

Fig. 2. Adding and deleting pORFs creates additional splice forms. (A) An ethidium bromide-stained acrylamide gel (lanes M, 1, and 2) and Southern blot autoradiograph (lanes 3 and 4) of the PCR products resulting from a nested PCR series using primers (25+44) and (26+44). The templates in the PCR were a control plasmid containing shal 1.e (lanes 1,3) or lobster nervous system cDNA (lanes 2,4). The Southern blot was probed with ^{32}-P labeled oligonucleotide 22. The sizes of the molecular weight standard (M) are indicated. (B) An acrylamide gel (lanes M, 1, and 2) and Southern blot (lanes 3 and 4) of the PCR products from two nested PCR series on lobster nervous system cDNA using primers (17+45) and (10+45), (lanes 1 and 3), or (17+46) and (10+46), (lanes 2 and 4). The Southern blot was probed with oligonucleotide 1. C. An acrylamide gel (lanes M, 1, 2, and 3) and Southern blot (lanes 4, 5, and 6) of the PCR products from three nested PCR series on lobster nervous system cDNA using primers (17+5) and (10+5), (lanes 1 and 4), or (17+46) and (10+46), (lanes 2 and 5), or (17+38) and (10+38), (lanes 3 and 6). The Southern blot was probed with oligonucleotide 40.

oligonucleotide 40:pORF C, thus indicating the existence of at least three additional transcripts (1.j, 1.k. 1.l). These experiments also indicated that shal 1.c transcripts can lack pORF P (shal 1.m), as seen in the faint, lower band in Fig. 2C, lanes 3 and 6. Using this same strategy we found that the lobster nervous system contains transcripts in which pORF G is inserted into the shal 1a transcript (shal 1.n). The results of all these experiments suggest a minimum of 14 alternately spliced *shal* transcripts. While we believe that we have identified the major species of *shal* transcripts in *Panulirus*, other splice forms most likely exist.

Characterizing and comparing the pORFs in the carboxy-termini

The amino acid sequences for all the alternately spliced pORFs, as well as putative sites of post translational modifications, are shown in Fig. 3A. The carboxy-terminus of a shal channel can contain between 1 and 15 putative phosphorylation sites depending upon the isoform. In Fig. 3B the carboxy-termini of the known full-length lobster shal isoforms are aligned with the shal (Kv4) proteins encoded by the three known human shal (Kv4) genes: hKv4.1, hKv4.2, and hKv4.3. This alignment begins at the very end of the well-conserved pORF A, which is represented by the peptide DKRKAQK. The intron/exon boundaries have been defined for the three human genes (Isbrandt et al., 2000), and amino acids representing the beginning and end of each exon are indicated by shaded circles in the human sequences. Fig. 3 illustrates that two alternate splice sites are conserved across species and genes (sites 1 and 2 in Fig. 1). The invariant pORF B is well conserved across species. However, most of the alternately spliced pORFs are not highly conserved and only lobster shal pORFs P, M, and N share significant homology with the mammalian proteins.

Lobster pORF P is 27–35% identical to the human proteins at the amino acid level. The length of this pORF is not conserved across species and the human version is significantly longer in all three genes. Perhaps as the human genes diverged and nonessential pORFs were reconfigured, splice sites were lost. Unlike the mammalian counterparts, lobster pORF P also contains a putative ATP/GTP-binding site (P-loop). Lobster pORF M is just as highly conserved across species and shows 19–37% identity to the mammalian shal (Kv4) proteins. Lobster pORF N is the most highly conserved of the alternately spliced pORFs, and is 38–50% identical to the mammalian proteins. Of the five carboxy-terminal pORFs (D, E, I, O, and N), only N shares homology with the mammalian sequences. The carboxy-terminal amino acids of some K^+ channels are responsible for channel clustering via interactions with proteins containing PDZ domains (Sheng and Pak, 2000). In the case of pORF N and the mammalian shal proteins, the binding motif would be: L/V-R/K-I/V-S-S/A-L. This consensus sequence is consistent with the requirements for a strong Group I PDZ-binding domain (Songyang et al., 1997). The other four lobster termini are not strong candidates for interactions with known PDZ domains, and transcripts containing these carboxy-termini may use targeting sequences located elsewhere in the carboxy tail (Lim et al., 2000). Interestingly, two of the five termini have a putative kinase site in the penultimate position (pORFs E and N). The phosphorylation state of this site regulates anchoring of the inward rectifier K^+ channel, KIR 2.3 (Cohen et al., 1996).

Characterizing shal isoforms in oocytes

Alternate splicing of the lobster *shaker* transcript produces at least 16 proteins. In this case, alternate exon usage produces structural changes in the α-subunits that lead to stable differences in the biophysical properties of the various homomeric shaker channels when expressed in oocytes (Kim et al., 1997, 1998). The alternately spliced carboxy-termini of lobster shal channels

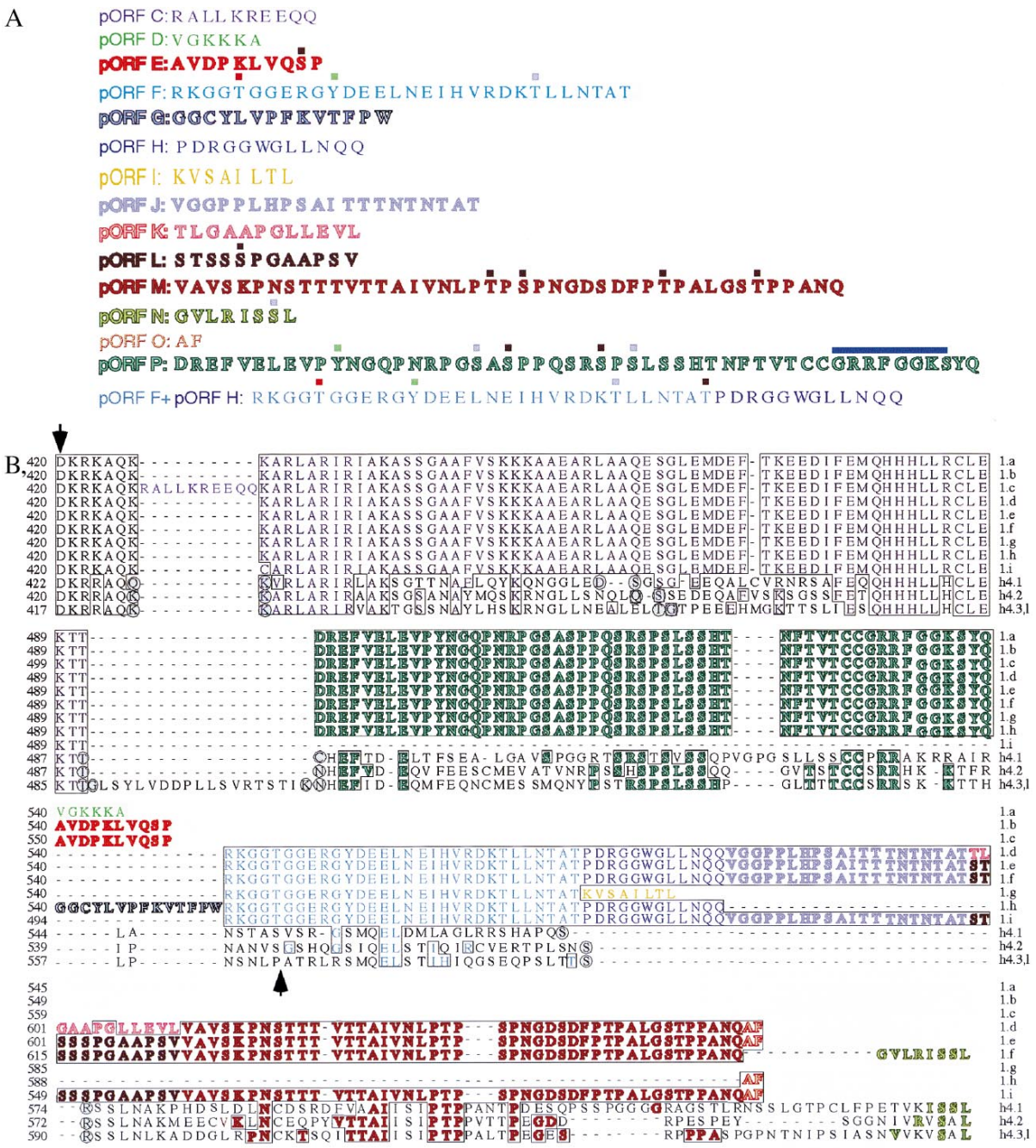

Fig. 3. Comparison of the pORFs in each lobster shal isoform with the human shal proteins. (A) Lobster shal pORFs and their post-translational modifications. The amino acid composition of each of the pORFs is indicated. Putative phosphorylation sites are represented as colored squares above the peptide sequence for individual pORFs and for the single case where a combination of two pORFs created a new site: casein kinase II (orange), mitogen-activated protein kinase (brown), calcium-calmodulin dependent kinase II (purple), tyrosine kinase (green). The P-loop, or ATP/GTP-binding site motif A, is indicated by a blue bar. (B) Alignment of the deduced amino acid sequences of the lobster isoforms shal 1.a–shal 1.i with the three human proteins Kv4.1, Kv4.2, and Kv4.3, long. The hKv4.3 transcript is alternately spliced, at alternate splice site 2. The long version is illustrated. The short version is identical except that it lacks the exon between pORFs B and P. The alignments begin with the last seven amino acids in pORF A. The number of the first amino acid on each line is indicated to the left of the alignment, where number 1 is the initiator methionine. Shaded circles indicate the amino acids at the beginning and the end of exons in the human proteins. Arrows mark the carboxy-terminal fast inactivation domain defined by Jerng and Covarrubias (1997). The color scheme is preserved from part A to B. Human amino acids that are identical to shal 1.e are boxed. All identical amino acids are colored appropriately. Accession numbers: NP_004970 (hKv4.1), CAB 56841 (hKv4.2), AAF 20924 (hKv4.3), L49135 [shal 1.a which was previously published in Baro et al., 1996). Note: there was a sequence misread in the original publication that altered the carboxy-terminus of the protein; this has since been corrected in the original GenBank submission and is shown in its corrected form here], AF375598, AF375599, AF375600, AF375601, AF375602, AF375603, AF375604, AF375605 (shal 1.b–shal 1.i, respectively).

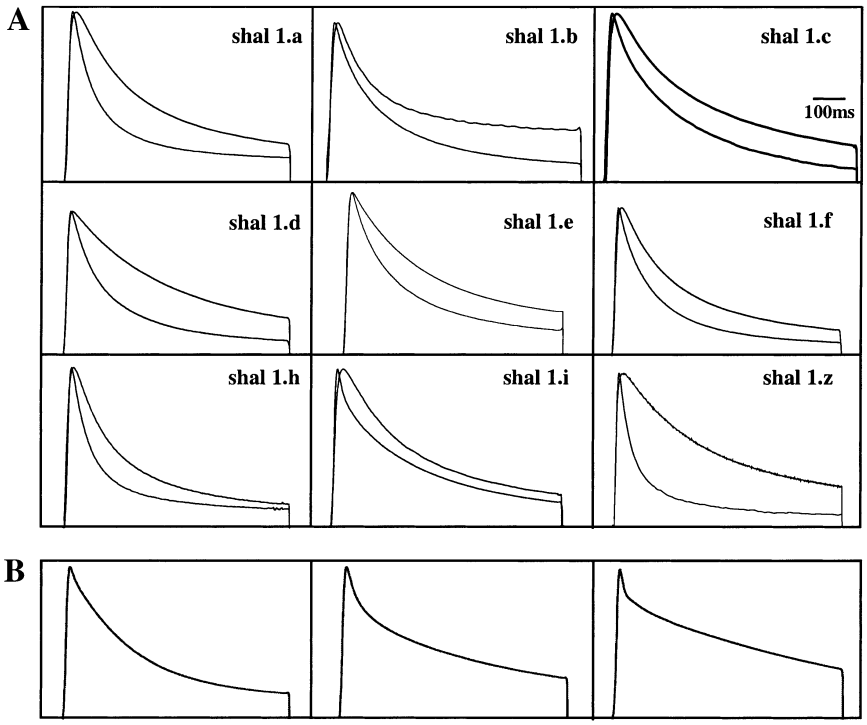

Fig. 4. (A) Current traces from lobster shal isoforms. The two traces in each panel are examples of the Type I and Type II currents produced by each shal isoform. Each of the two traces was obtained from a different oocyte injected with the same RNA, and stepped to +20 mV after a prepulse to −90 mV. Type II currents always show slower inactivation kinetics. Currents were elicited as described in Experimental procedures. For each set of traces, currents were plotted, scaled to the same peak amplitude, and overlaid. (B) Further examples of Type I currents produced by shal 1.e injected on the same day into oocytes donated by the same frog and recorded 3 days later. Note the variability in isoform expression in different oocytes.

contain one of the two domains that co-operatively mediate fast inactivation of shal channels (Jerng and Covarrubias, 1997; Jerng et al., 1999). Thus, we hypothesized that alternate splicing could generate structural differences in shal α-subunits that result in stable differences in inactivation kinetics between isoforms, and that this could account for the 10-fold difference in the inactivation time constants of pyloric I_As. To test this hypothesis we constructed full-length transcripts for nine shal isoforms (Fig. 1). RNA was transcribed from each of these constructs and injected into *Xenopus* oocytes to create homomeric shal channels.

As expected, shal isoforms expressed in *Xenopus* oocytes gave rise to outward K^+ currents that decayed over a multi-exponential time course. Like mouse shal currents (Jerng and Covarrubias 1997; Jerng et al., 1999), lobster shal currents expressed in oocytes displayed three time constants of inactivation. However, each isoform demonstrated a remarkable amount of variability between oocytes in both their time constants and the relative contributions of each component to the peak current (Figs. 4 and 5). The data suggest that the inactivation kinetics of shal channels are differentially regulated depending upon the individual oocyte. Fig. 4 illustrates the range of currents that a single isoform produced in separate oocytes, even from the same frog and recorded on the same day. The currents produced by any given isoform could be broadly classified into two types, with a great deal of variability within each class (Fig. 4B). Type I currents inactivated with three time constants of inactivation (τ_1–τ_3) over a 4-s test pulse, while Type II currents lacked τ_1 but possessed τ_2 and τ_3. Elimination of rapid inactivation from Type II currents also delayed the time to peak current (Fig. 4A). This same effect is seen in mouse shal (Kv4.1) channels when the fast inactivation domain(s) is deleted, and most probably represents channels that would otherwise be inactivated, now contributing to the peak, and/or a change in the voltage dependence or rate of activation (Jerng and Covarrubias 1997; Jerng et al., 1999). The

Table 2. Time constants of inactivation

Isoform	τ_{fast}	$\tau_{intermediate}$	τ_{slow}
shal 1.a	65 ± 23[3] (13)	327 ± 72 (13)	ND
shal 1.b	86 ± 10[5,9,10] (12)	341 ± 047 (12)	ND
shal 1.c	103 ± 35[1,5,9,10] (9)	389 ± 131 (14)	894 ± 138 (5)
shal 1.d	72 ± 31 (12)	332 ± 54 (12)	ND
shal 1.e	46 ± 25[2,3] (25)	362 ± 108 (27)	874 ± 169 (7)
shal 1.f	78 ± 31 (14)	381 ± 112[8] (13)	1039 ± 253 (3)
shal 1.h	69 ± 24 (6)	227 ± 84[6,9,10] (9)	969 ± 379 (6)
shal 1.i	54 ± 33[2,3] (27)	387 ± 88[8] (27)	ND
shal 1.z	54 ± 29[2,3] (38)	384 ± 147[8] (41)	865 ± 90 (13)

Values on the top line represent means ± S.D.; *n* is reported in parentheses. Significantly different ($P < 0.05$) than [1]1.a, [2]1.b, [3]1.c, [4]1.d, [5]1.e, [6]1.f, [8]1.h, [9]1.i, [10]1.z. ND, not determined: only 1-s test pulses were performed (see main text for explanation).

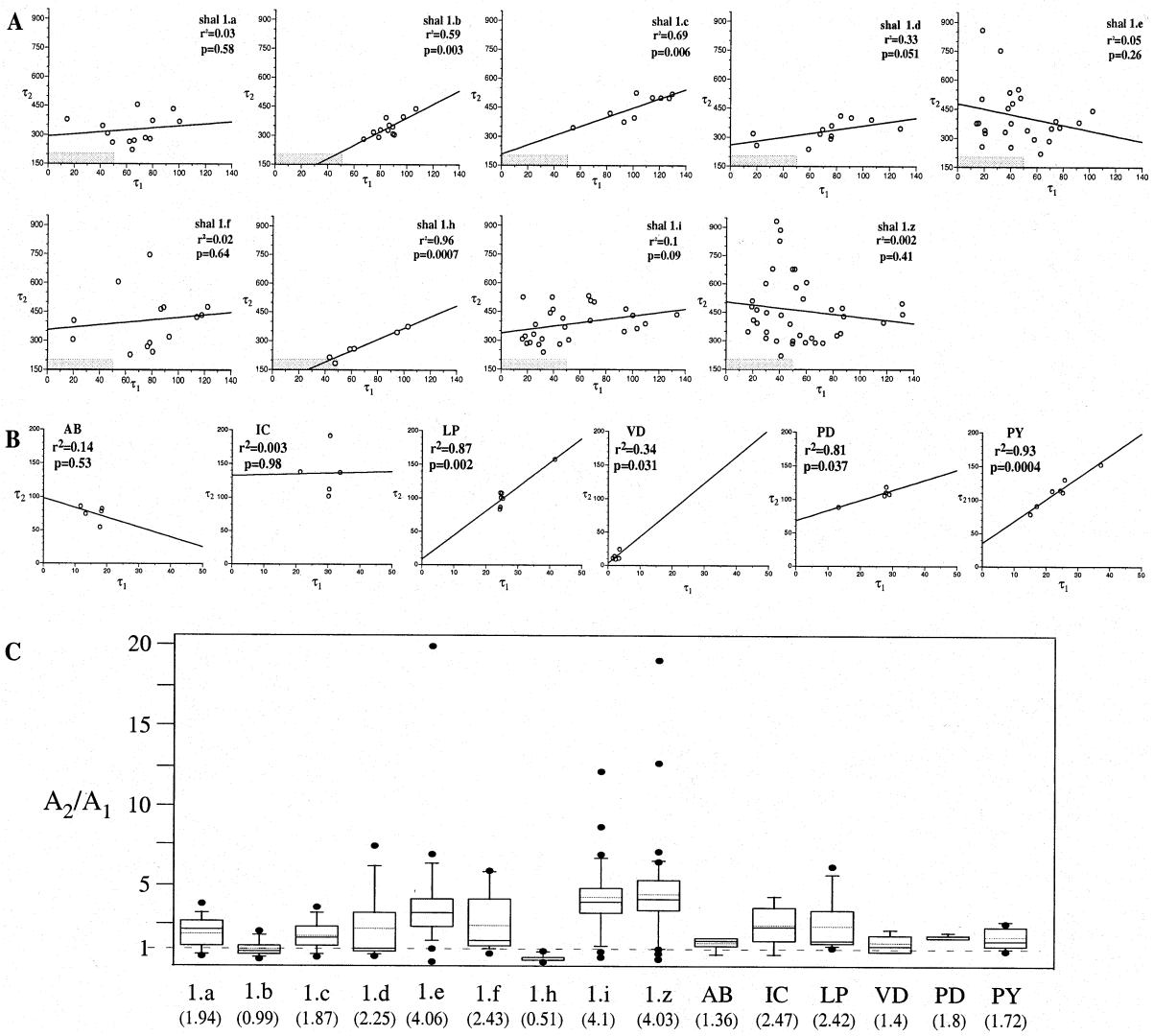

Fig. 5. Comparison of the kinetic properties of shal channels expressed in oocytes and pyloric neurons. (A) Plots of τ_2 versus τ_1 for all Type I currents. Each circle represents the time constants for the macroscopic Type I current elicited from a single oocyte in response to a hyperpolarizing prepulse to −90 mV followed by a 1-s test pulse to +20 mV as described in Experimental procedures. Data from all frogs injected with the same isoform are pooled and represented in each panel. Lines represent simple regressions of all data points. The r^2 and P values for the correlation are as indicated. Shaded regions represent the area of overlap with the values for pyloric neurons shown in B. (B) Plots of τ_2 versus τ_1 for isolated shal currents obtained from five to seven neurons in each pyloric cell type. The six pyloric cell types and the number of cells in each pyloric cell type are: PD, pyloric dilator (2); VD, ventricular dilator (1); PY, pyloric constrictor (8); AB, anterior burster (1); IC, inferior cardiac (1); LP, lateral pyloric (1). Each circle represents the time constants of the macroscopic I_A elicited by a hyperpolarizing prepulse followed by a 500-ms test pulse from a single, identified pyloric neuron. Lines represent linear regressions of the data points. The r^2 and P values for the correlation are as indicated. Data were taken from Baro et al. (1997). (C) Box plots showing the distribution of A_2/A_1 for all Type I currents shown in A and B. Black horizontal lines of a box represent the 25th, 50th, and 75th percentile points. Whiskers represent the 10th and 90th percentile points, filled circles indicate outliers, and dotted lines represent the means. The mean is also written in parentheses underneath the name of the isoform or cell type.

extent of the variability of Type I currents is illustrated in Fig. 5A where τ_2 is plotted against τ_1 for all currents recorded for a given isoform. Depending upon the isoform, τ_1 could vary by as much as a factor of eight (1.i and 1.z) and τ_2 could vary by up to a factor of 4.2 (1.z). Box plots of A_2/A_1 summarize the variation in the fractional amplitudes of τ_2 relative to τ_1 (Fig. 5C), and illustrate that the relative amounts of the fast and slowly inactivating components are differentially regulated so that either component can dominate a Type I current. Fig. 5 and Table 2 demonstrate that the inactivation parameters for different shal splice forms are broadly overlapping so that there are few significant differences in inactivation kinetics between shal isoforms. Alternate exon usage generates few stable changes in shal α-sub-

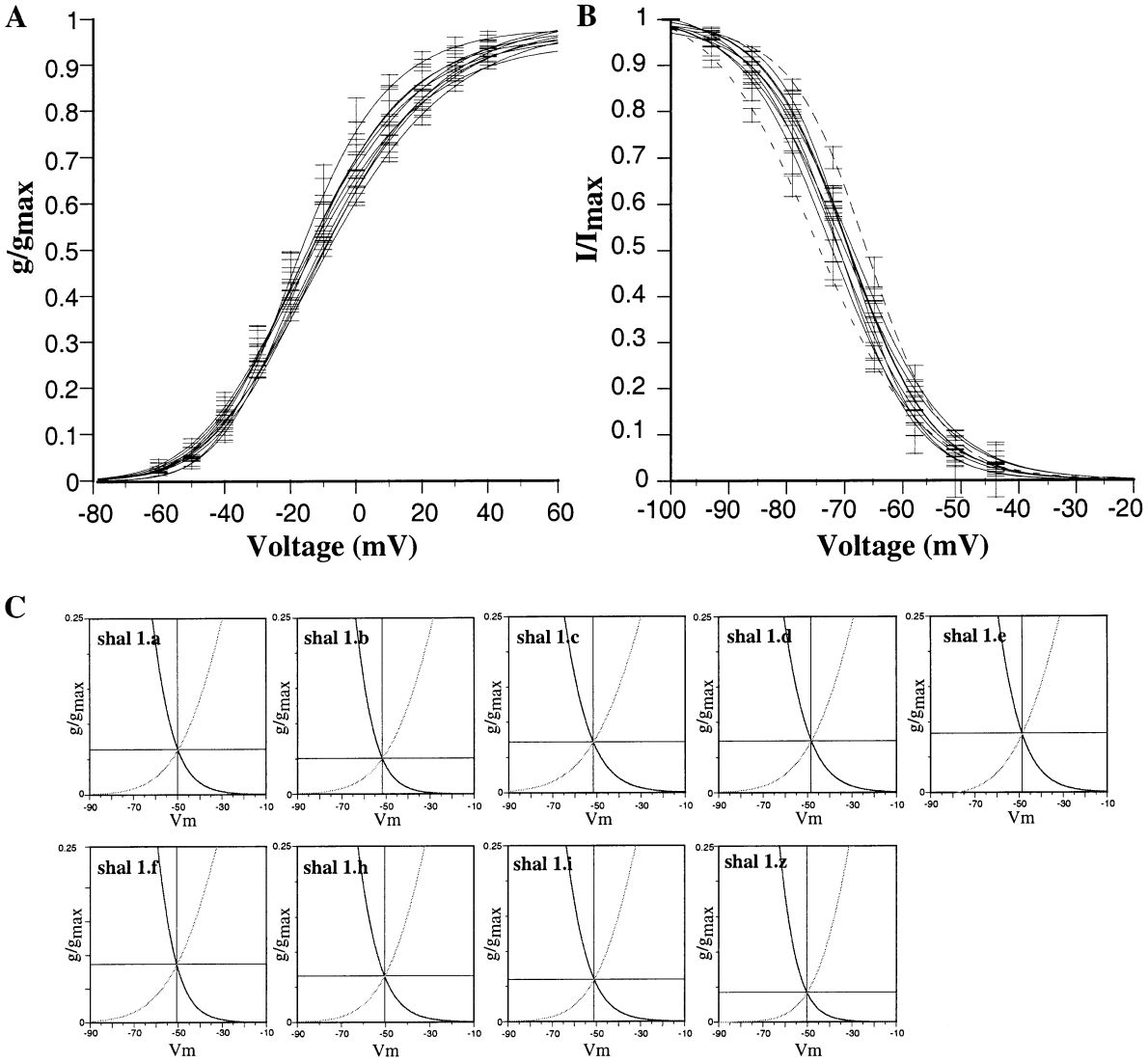

Fig. 6. Voltage dependence of shal isoforms. (A) Peak conductance/voltage relationships for activation of the shal isoforms. Activation curves are least squares fits to the third order Boltzmann equation described in Experimental procedures. Each set of data points is the average from a number of oocytes from at least two different frogs. The number of cells used to determine the average data set is given in Table 3. Bars represent the S.E.M. at each data point. (B) Steady-state inactivation of shal isoforms. Inactivation curves are least squares fits to first order Boltzmann equations. The dashed lines represent the two extreme isoforms, 1.c and 1.f. C. Steady-state window currents for shal isoforms. Window currents were obtained by plotting the activation and inactivation curves for each isoform on the same graph. Only the portion of plot containing the window current is shown.

unit structure that result in fixed differences in the inactivation kinetics of the different isoforms.

The voltage dependence of the shal isoforms expressed in oocytes showed similar variability to that described above. The voltages of half activation (V_{act}) for individual currents obtained from different oocytes injected with the same isoform varied by up to 20 mV. As a result, there were no significant differences in the average V_{act} between the different shal isoforms (Fig. 6A and Table 3). Similarly, while the slope factors could vary by roughly a factor of three between currents from different oocytes injected with the same isoform (11–38 mV, activation; 4.3–13.2 mV, inactivation), the average slope factors were for the most part not significantly different between isoforms (Table 3). Finally, the voltages of half inactivation (V_{inact}) varied by approximately 15 mV within an isoform. The average V_{inact} varied by 9 mV between isoforms, but only one isoform (shal 1.c) was significantly different from any of the others (Fig. 6B, Table 3). Fig. 6C illustrates that the peak amplitudes of the steady-state window currents vary with the splice form, and the steady-state conductances at the peak voltages vary significantly between 0.0002 (1.z) to 0.007 (1.e) percent of the total current. There are only slight differences in the peak voltages of the window currents (<4 mV), though the voltage ranges significantly expand and contract with the splice form.

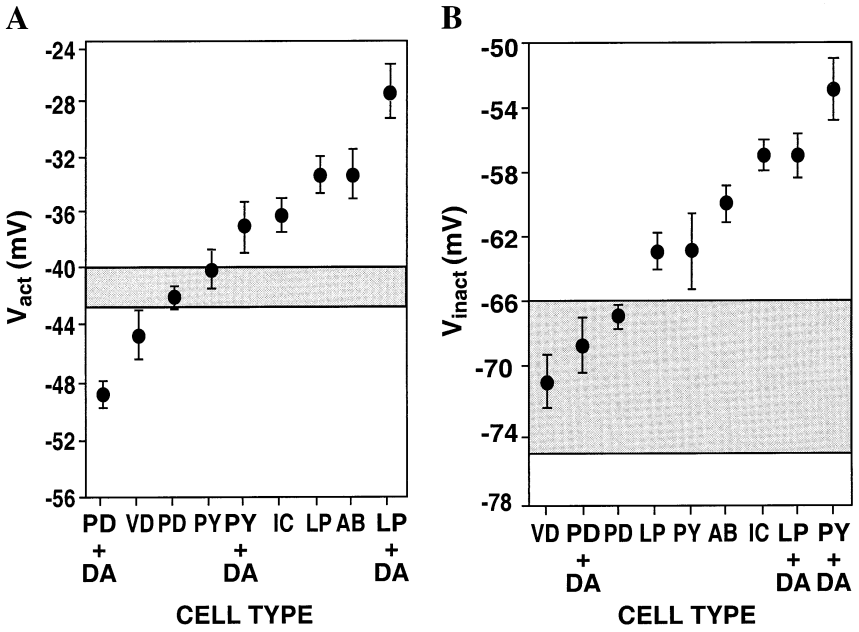

Fig. 7. Comparison of the voltage dependence of pyloric I_As with the various shal isoforms. The shaded area represents the range of the average voltage of half activation (A) or inactivation (B) exhibited by the shal isoforms expressed in oocytes (Table 3). Filled circles represent the average voltage of half activation (A) or inactivation (B) for each pyloric cell type as determined by two electrode voltage clamp from the neuronal soma. Synaptically isolated cells were recorded in the absence of neuromodulators or in the presence of 10^{-4} M bath applied dopamine (+DA). Data for pyloric cells were taken from (Harris-Warrick et al., 1995a,b; Baro et al., 1997; Kloppenburg et al., 1999) Bars represent ±S.E.M.

Alternate splicing alone cannot account for differences in pyloric I_As

We asked whether alternate splicing by itself could account for the 10-fold difference in I_A inactivation kinetics between pyloric cell types (Fig. 5B). Previous studies on pyloric I_As demonstrated that I_A inactivated almost completely over a 500-ms test pulse, and that τ_1 and τ_2 contributed substantially to inactivation, while τ_3 was undetectable (Baro et al., 1997). Thus, we compared τ_1 and τ_2 from pyloric I_As with Type I currents from shal isoforms expressed in oocytes. Plots of τ_2 vs. τ_1 for 5–7 neurons in each pyloric cell type are shown in Fig. 5B, and box plots of the A_2/A_1 ratio are given in Fig. 5C. Notice the difference in the scales of Fig. 5A, B: the gray shaded regions in Fig. 5A indicate the area represented by the plots in Fig. 5B. Except for one data point (1.h) there is no overlap between the plots of shal channels expressed in pyloric cells and oocytes. Interestingly, the variability in both τ_1 and τ_2 is greatly reduced in pyloric cells relative to oocytes, consistent with the idea that the cellular milieu is more stable in differentiated adult cell types under baseline conditions (no synaptic interactions and no neuromodulators present). However, differential modulation of shal currents still occurs in pyloric neurons and appears to vary with the cell type. For example, the time constants appear to co-vary in the pyloric constrictor (PY), pyloric dilator (PD), ventricular dilator (VD) and lateral pyloric (LP) cells, but not the inferior cardiac (IC) and LP [anterior burster (AB)] cells. Similarly, while the slow component always dominates pyloric shal currents, A_2/A_1 is differentially regulated in certain cell types like the IC and LP, but quite stable in other cell types like the PD

Table 3. Voltage dependence of shal isoforms

Isoform	V_{act}	Activation slope	V_{inact}	Inactivation slope
shal 1.a	−41 ± 1.0 (22)	22 ± 0.9 (22)	−69 ± 0.6[3] (27)	6.8 ± 0.2[3] (27)
shal 1.b	−40 ± 1.3 (11)	22 ± 0.7 (11)	−71 ± 1.4 (13)	6.8 ± 0.7 (13)
shal 1.c	−42 ± 1.0 (20)	24 ± 1.0[10] (20)	−75 ± 0.7[1,5,6,10] (29)	8.7 ± 0.4[1,6,10] (29)
shal 1.d	−40 ± 2.5 (8)	22 ± 1.2 (8)	−69 ± 2.2 (9)	7.5 ± 0.6 (9)
shal 1.e	−42 ± 1.5 (15)	23 ± 1.4 (15)	−68 ± 1.1[3] (17)	7.6 ± 0.5 (17)
shal 1.f	−43 ± 1.7 (13)	22 ± 0.9 (13)	−66 ± 0.8[3] (12)	6.4 ± 0.3[3] (12)
shal 1.h	−43 ± 2.3 (8)	21 ± 1.2 (8)	−72 ± 1.4 (8)	6.9 ± 0.9 (8)
shal 1.i	−42 ± 2.1 (7)	21 ± 2.3 (7)	−70 ± 2 (7)	7.5 ± 0.5 (7)
shal 1.z	−40 ± 1.3 (9)	18 ± 0.9[3] (9)	−69 ± 0.7[3] (12)	6.2 ± 0.4[3] (12)

Values represent means ± S.E.M. Significantly different ($P < 0.05$) than [1]1.a, [2]1.b, [3]1.c, [4]1.d, [5]1.e, [6]1.f, [8]1.h, [9]1.i, [10]1.z. n is reported in parentheses.

(Fig. 5C). The data suggest that alternate splicing alone does not generate stable alterations in the structure of the shal α-subunit that could underlie the 10-fold difference in the inactivation kinetics between pyloric neurons.

Likewise, alternate splicing alone does not result in stable structural changes that could account for baseline differences in the voltage dependence of pyloric I_As. Fig. 7 compares isoform variability in voltage dependence to that observed in pyloric I_As. The voltages of half activation and inactivation for the different pyloric I_As vary continuously between two extremes. When recording under baseline conditions, where pyloric neurons are synaptically isolated and no neuromodulators are in the bath, the average V_{act}s for the six pyloric I_As vary by up to 14 mV, and this range can be further extended by neuromodulators like dopamine (Harris-Warrick et al., 1995a,b; Kloppenburg et al., 1999), which presumably act by a second messenger mediated modification of channel charge or structure (Fig. 7A). The average V_{act}s for the nine shal isoforms expressed in oocytes occupy just a small 4-mV segment on the continuum. The voltage dependence of all heterotetramers would most likely also fall within this 4-mV voltage range. The average pyloric I_A V_{inact}s also vary by 14 mV under baseline conditions and can also be modulated by dopamine (Fig. 7B). The range of average values displayed by the shal isoforms expressed in oocytes is similar (9 mV), but as a whole the values are more hyperpolarized.

The steady-state window I_As of pyloric neurons vary significantly with respect to peak voltage and amplitude (Baro et al., 1997). The peak amplitudes of the pyloric window currents spanned the same range observed for shal isoforms expressed in oocytes; however, the peak voltages of the shal isoform window currents expressed in oocytes did not represent the range observed for pyloric neurons. Only the peak voltage of the VD and PD steady-state currents (−50 mV) resembled those of shal isoforms expressed in oocytes. The significantly depolarized shifts in the peak voltages observed in the other four pyloric window currents were not reproduced by alternate splicing (average peak voltages ranged from −35 mV to −50 mV depending on the pyloric cell type; Baro et al., 1997). In all cases the voltage range of the pyloric window currents was less broad than shal isoforms expressed in oocytes.

DISCUSSION

There are at least eight points of alternate splicing that divide the lobster *shal* transcript into 16 pORFs (A–P). Every channel contains pORFs A and B, which make up 70–97% of the protein, depending upon the splice form. A 10 amino acid segment (pORF C) may interrupt these two invariant regions. Every isoform also contains a variable carboxy-terminus made from some combination of pORFs D–P. The termini range from 10 to 191 amino acids in length, and contain from 1 to 15 putative phosphorylation sites. Each shal isoform has the ability to create a broad spectrum of currents, and ultimately, the current produced depends upon the cellular environment. While we have not yet determined the isoform expression pattern in pyloric neurons, the present study illustrates that stable differences in the baseline I_A between pyloric cell types cannot simply be due to cell-specific patterns of *shal* splicing that yield structurally different isoforms with fixed differences in their biophysical properties. However, alternate splicing could indirectly contribute to pyloric I_A diversity.

Ion channel α-subunits interact with ancillary proteins like β-subunits (Rettig et al., 1994), γ-subunits (Jegla and Salkoff, 1997), KCHIPs (An et al., 2000), and MiRPs (Abbott et al., 1999). These interactions can alter channel properties and create positional diversity among cell types (Ramanathan et al., 1999). Thus, isoform-specific interactions with auxiliary proteins could theoretically lead to I_A diversity. KCHIP and γ-subunits interactions with shal (Kv4) α-subunits are determined by the invariant portion of the shal channel; however, β-subunits have recently been shown to interact with the carboxy-termini of shal (Kv4) subunits (Yang et al., 2001). Thus, it is possible that lobster shal isoform-specific interactions with ancillary β-subunits could contribute to pyloric I_A diversity.

Since the type and number of phosphorylation sites vary with the lobster shal isoform, modifications by second messenger systems leading to α-subunit phosphorylation could also regulate the kinetics of inactivation in an isoform-specific manner and lead to pyloric I_A diversity. This idea is consistent with: (1) previous studies showing that the carboxy-terminus is involved in inactivation (Jerng and Covarrubias, 1997; Jerng et al., 1999), (2) the variability in inactivation kinetics displayed by a single lobster shal isoform, and (3) a study by Tsunoda and Salkoff (1995), which demonstrated that shal currents in *Drosophila* embryonic neurons showed a >100-fold variation in τ_f, and that a single channel could spontaneously alter τ_f by more than a factor of ten during the recording period.

However, it seems less likely that alternate splicing is involved in establishing differences in the voltage dependence of gating. It is generally thought that the voltage sensor of all Shaker family proteins includes amino acids in S2, S3, S4, the S4–S5 loop, and the P loop (Perozo and Bezanilla, 1990; Papazian et al., 1995; Planells-Cases et al., 1995; Aggarwal and MacKinnon, 1996; Seoh et al., 1996). Thus, the voltage sensor is located in the invariant pORF A (Fig. 1). Perozo and Bezanilla (1990) demonstrated that phosphorylation could increase the density of surface charges in the vicinity of the voltage sensor and shift its voltage dependence toward more depolarized potentials. In our study, the midpoint potentials for a given isoform expressed in oocytes could vary by up to 20 mV, so that the V_{act} for shal isoforms expressed in oocytes ranged from −31 mV to −56 mV, and the V_{inact} from −59 to −82 mV. These ranges are similar to the pyloric cell activation and inactivation continua shown in Fig. 7. One interpretation of these data is that changes in the phosphorylation state of the population of shal channels alter the average midpoint

potentials for the macroscopic I_A. The regions housing the voltage sensor in lobster shal channels contain putative phosphorylation sites (Baro et al., 1996). In the simplest case, a constitutive cycle of phosphorylation and dephosphorylation at just one of these sites could regulate the V_{act} and produce the entire activation continuum observed in Fig. 7. For example, when 100% of the subunits in the population are phosphorylated, the average V_{act} might be −24 mV, while dephosphorylating 100% of the subunits would change the average V_{act} to −56 mV. In this case, if 50% of the subunits were phosphorylated, the average V_{act} for the population of channels would be −40 mV, though voltage dependence at the single channel level could be very diverse. Changing the rates of constitutive phosphorylation and dephosphorylation at this site via typical second messenger cascades could produce the entire activation continuum shown in Fig. 7. Unlike oocytes, mature pyloric neurons would consistently regulate the phosphorylation state of this site under baseline conditions in a cell-specific manner, and neuromodulators like dopamine would alter that state in reproducible ways. Of course, multiple phosphorylation sites might participate in determining the voltage dependence of gating, and a single site might alter multiple parameters. In any event, differences in pyloric I_A voltage dependence under baseline conditions may reflect cell-specific differences in second messenger set points, differences in the components and concentrations of second messenger cascades, or cell-specific differences in auxiliary subunit interactions, rather than structural differences in α-subunits.

Roles of alternate splicing

As implied above, one of the main functions of alternate splicing may be to introduce different phosphorylation sites that allow the various isoforms to be differentially regulated. Indeed, alternate splicing has been shown to alter BK channel sensitivity to protein kinase A phosphorylation (Tian et al., 2001). Since ion channel isoforms are often expressed in a cell-specific manner (Atkinson et al., 2000; Bohm et al., 2000; Brenner et al., 2000), differential expression of shal isoforms among pyloric neurons could result in the differential modulation of I_A in the various cell types. If two or more isoforms were expressed in the same cell type, the formation of heteromeric channels could increase the ability of different neuromodulators to influence the channels. Alternatively, differential targeting of homomeric channels might produce localized differences in the modulation of I_A within a single cell.

Alternate splicing of the 3′UTR could also function to differentially localize *shal* mRNA (Rook et al., 2000), or differentially regulate post-transcriptional gene expression (Decker and Parker, 1995). At the protein level, short sequences in the carboxy-termini of receptor and channel proteins are responsible for the compartmentalization and clustering of these proteins (Arnold and Clapham, 1999; Stowell and Craig, 1999; Lim et al., 2000). Alternate splicing could change the scaffold to which shal channels attach, and/or the makeup of the proteins in the shal cluster, and/or the compartmentalization of the channels. Finally, it is possible that the different carboxy-termini alter biophysical characteristics not examined in this study, or possess specialized functions unrelated to the biophysical properties of the channel. For example, Qian and Pfaffinger (1999) suggested that the carboxy-termini of shal channels might be involved in communicating membrane events to the nucleus. They hypothesized that the carboxy-terminus of the rat shal channel (Kv4.2) could be cleaved in response to extracellular signals and translocate to the nucleus where it could affect transcription. Thus, alternate splicing may confer as yet undiscovered functions to the different shal isoforms.

Acknowledgements—We thank Drs. W. Krenz and A. Selverston for the temporary use of their equipment, and Drs. L.F. Santana and J. Peck for useful discussions of the data. M.R. was supported by the Institute of Neurobiology summer undergraduate internship program. This work was supported by NIH RO1 Grants NS38770 (D.J.B.) and NS35631 (R.H.W.), RCMI-UPR G12RR-03051 (D.J.B.), and NSF-EPSCoR (D.J.B.).

REFERENCES

Abbott, G.W., Sesti, F., Splawski, I., Buck, M.E., Lehmann, M.H., Timothy, K.W., Keating, M.T., Goldstein, S.A., 1999. MiRP1 forms I_{Kr} potassium channels with HERG and is associated with cardiac arrhythmia. Cell 97, 175–187.

Aggarwal, S.K., MacKinnon, R., 1996. Contribution of the S4 segment to gating charge in the Shaker K+ channel. Neuron 16, 1169–1177.

An, W., Bowlby, M., Betty, M., Cao, J., Ling, H.-P., Mendoza, G., Hinson, J., Mattson, K., Strassle, B., Trimmer, J., Rhodes, K., 2000. Modulation of A-type potassium channels by a family of calcium sensors. Nature 403, 553–556.

Arnold, D.B., Clapham, D.E., 1999. Molecular determinants for subcellular localization of PSD-95 with an interacting K+ channel. Neuron 23, 149–157.

Atkinson, N.S., Brenner, R., Chang, W., Wilbur, J., Larimer, J.L., Yu, J., 2000. Molecular separation of two behavioral phenotypes by a mutation affecting the promoters of a Ca-activated K channel. J. Neurosci. 20, 2988–2993.

Ausubel, F., Brent, R., Kinston, R., Moore, D., Seidman, J., JA, J.S., Struhl, K. 1990. Current Protocols in Molecular Biology. Greene Publishing Associates and Wiley Interscience, New York.

Baro, D.J., Ayali, A., French, L., Scholz, N.L., Labenia, J., Lanning, C.C., Graubard, K., Harris-Warrick, R.M., 2000. Molecular underpinnings of motor pattern generation: Differential targeting of shal and shaker in the pyloric motor system. J. Neurosci. 20, 6619–6630.

Baro, D.J., Cole, C.L., Zarrin, A.R., Hughes, S., Harris-Warrick, R.M., 1994. Shab gene expression in identified neurons of the pyloric network in the lobster stomatogastric ganglion. Recept. Channels 2, 193–205.

Baro, D.J., Coniglio, L.M., Cole, C.L., Rodriguez, H.E., Lubell, J.K., Kim, M.T., Harris-Warrick, R.M., 1996. Lobster shal: comparison with *Drosophila* shal and native potassium currents in identified neurons. J. Neurosci. 16, 1689–1701.

Baro, D.J., Levini, R.M., Kim, M.T., Willms, A.R., Lanning, C.C., Rodriguez, H.E., Harris-Warrick, R.M., 1997. Quantitative single-cell-reverse transcription-PCR demonstrates that A-current magnitude varies as a linear function of shal gene expression in identified stomatogastric neurons. J. Neurosci. 17, 6597–6610.
Bohm, R.A., Wang, B., Brenner, R., Atkinson, N.S., 2000. Transcriptional control of Ca(2+)-activated K(+) channel expression: identification of a second, evolutionarily conserved, neuronal promoter. J. Exp. Biol. 203, 693–704.
Brenner, R., Yu, J.Y., Srinivasan, K., Brewer, L., Larimer, J.L., Wilbur, J.L., Atkinson, N.S., 2000. Complementation of physiological and behavioral defects by a slowpoke Ca(2+)-activated K(+) channel transgene. J. Neurochem. 75, 1310–1319.
Cohen, N.A., Brenman, J.E., Snyder, S.H., Bredt, D.S., 1996. Binding of the inward rectifier K+ channel Kir 2.3 to PSD-95 is regulated by protein kinase A phosphorylation. Neuron 17, 759–767.
Decker, C.J., Parker, R., 1995. Diversity of cytoplasmic functions for the 3′ untranslated region of eukaryotic transcripts. Curr. Opin. Cell Biol. 7, 386–392.
Fettiplace, R., Fuchs, P.A., 1999. Mechanisms of hair cell tuning. Annu. Rev. Physiol. 61, 809–834.
Frohman, M. 1990. RACE: Rapid Amplification of cDNA Ends. In: Innis, M., Gelfand, D., Sninsky, J., White, T. (Eds.), PCR Protocols. Academic Press, San Diego, CA, pp. 28–38.
Graubard, K., Hartline, D.K., 1991. Voltage clamp analysis of intact stomatogastric neurons. Brain Res. 557, 241–254.
Harris-Warrick, R.M., Coniglio, L.M., Barazangi, N., Guckenheimer, J., Gueron, S., 1995a. Dopamine modulation of transient potassium current evokes phase shifts in a central pattern generator network. J. Neurosci. 15, 342–358.
Harris-Warrick, R.M., Coniglio, L.M., Levini, R.M., Gueron, S., Guckenheimer, J., 1995b. Dopamine modulation of two subthreshold currents produces phase shifts in activity of an identified motoneuron. J. Neurophysiol. 74, 1404–1420.
Hartline, D.K., 1979. Pattern generation in the lobster (*Panulirus*) stomatogastric ganglion. II Pyloric network simulation. Biol. Cybern. 33, 223–236.
Innis, M., Gelfand, D., Sninsky, J. (Eds.) 1995. PCR Stategies. Academic Press, San Diego, CA.
Innis, M., Gelfand, D., Sninsky, J., White, T. (Eds.) 1990. PCR Protocols. Academic Press, San Diego, CA.
Isbrandt, D., Leicher, T., Waldschutz, R., Zhu, X., Luhmann, U., Michel, U., Sauter, K., Pongs, O., 2000. Gene structures and expression profiles of three human KCND (Kv4) potassium channels mediating A-type currents I(TO) and I(SA). Genomics 64, 144–154.
Jegla, T., Salkoff, L., 1997. A novel subunit for shal K+ channels radically alters activation and inactivation. J. Neurosci. 17, 32–44.
Jerng, H.H., Covarrubias, M., 1997. K+ channel inactivation mediated by the concerted action of the cytoplasmic N- and C-terminal domains. Biophys. J. 72, 163–174.
Jerng, H.H., Shahidullah, M., Covarrubias, M., 1999. Inactivation gating of Kv4 potassium channels: molecular interactions involving the inner vestibule of the pore. J. Gen. Physiol. 113, 641–660.
Jones, E.M., Gray-Keller, M., Art, J.J., Fettiplace, R., 1999a. The functional role of alternative splicing of Ca(2+)-activated K+ channels in auditory hair cells. Ann. N. Y. Acad. Sci. 868, 379–385.
Jones, E.M., Gray-Keller, M., Fettiplace, R., 1999b. The role of Ca2+-activated K+ channel spliced variants in the tonotopic organization of the turtle cochlea. J. Physiol. Lond. 518, 653–665.
Kim, M., Baro, D.J., Lanning, C.C., Doshi, M., Farnham, J., Moskowitz, H.S., Peck, J.H., Olivera, B.M., Harris-Warrick, R.M., 1997. Alternative splicing in the pore-forming region of shaker potassium channels. J. Neurosci. 17, 8213–8224.
Kim, M., Baro, D.J., Lanning, C.C., Doshi, M., Moskowitz, H.S., Farnham, J., Harris-Warrick, R.M., 1998. Expression of *Panulirus* shaker potassium channel splice variants. Recept. Channels 5, 291–304.
Kloppenburg, P., Levini, R.M., Harris-Warrick, R.M., 1999. Dopamine modulates two potassium currents and inhibits the intrinsic firing properties of an identified motor neuron in a central pattern generator network. J. Neurophysiol. 81, 29–38.
Lim, S.T., Antonucci, D.E., Scannevin, R.H., Trimmer, J.S., 2000. A novel targeting signal for proximal clustering of the Kv2.1 K+ channel in hippocampal neurons. Neuron 25, 385–397.
Navaratnam, D.S., Bell, T.J., Tu, T.D., Cohen, E.L., Oberholtzer, J.C., 1997. Differential distribution of Ca2+-activated K+ channel splice variants among hair cells along the tonotopic axis of the chick cochlea. Neuron 19, 1077–1085.
Oberholtzer, J.C., 1999. Frequency tuning of cochlear hair cells by differential splicing of BK channel transcripts. J. Physiol. Lond. 518, 629.
Papazian, D.M., Shao, X.M., Seoh, S.A., Mock, A.F., Huang, Y., Wainstock, D.H., 1995. Electrostatic interactions of S4 voltage sensor in Shaker K+ channel. Neuron 14, 1293–1301.
Perozo, E., Bezanilla, F., 1990. Phosphorylation affects voltage gating of the delayed rectifier K+ channel by electrostatic interactions. Neuron 5, 685–690.
Planells-Cases, R., Ferrer-Montiel, A.V., Patten, C.D., Montal, M., 1995. Mutation of conserved negatively charged residues in the S2 and S3 transmembrane segments of a mammalian K+ channel selectively modulates channel gating. Proc. Natl. Acad. Sci. USA 92, 9422–9426.
Qian, Y., Pfaffinger, P., 1999. The N-terminal and C-terminal domain of voltage dependent potassium channels are processed and may act as signaling molecules. Soc. Neurosci. Abstr. 25, 531.
Ramanathan, K., Michael, T.H., Jiang, G.J., Hiel, H., Fuchs, P.A., 1999. A molecular mechanism for electrical tuning of cochlear hair cells. Science 283, 215–217.
Rettig, J., Heinemann, S.H., Wunder, F., Lorra, C., Parcej, D.N., Dolly, J.O., Pongs, O., 1994. Inactivation properties of voltage-gated K+ channels altered by presence of beta-subunit. Nature 369, 289–294.
Rook, M.S., Lu, M., Kosik, K.S., 2000. CaMKIIalpha 3′ untranslated region-directed mRNA translocation in living neurons: visualization by GFP linkage. J. Neurosci. 20, 6385–6393.
Rosenblatt, K.P., Sun, Z.P., Heller, S., Hudspeth, A.J., 1997. Distribution of Ca2+-activated K+ channel isoforms along the tonotopic gradient of the chicken's cochlea. Neuron 19, 1061–1075.
Seoh, S.A., Sigg, D., Papazian, D.M., Bezanilla, F., 1996. Voltage-sensing residues in the S2 and S4 segments of the Shaker K+ channel. Neuron 16, 1159–1167.
Sheng, M., Pak, D.T., 2000. Ligand-gated ion channel interactions with cytoskeletal and signaling proteins. Annu. Rev. Physiol. 62, 755–778.
Songyang, Z., Fanning, A.S., Fu, C., Xu, J., Marfatia, S.M., Chishti, A.H., Crompton, A., Chan, A.C., Anderson, J.M., Cantley, L.C., 1997. Recognition of unique carboxyl-terminal motifs by distinct PDZ domains. Science 275, 73–77.
Stowell, J.N., Craig, A.M., 1999. Axon/dendrite targeting of metabotropic glutamate receptors by their cytoplasmic carboxy-terminal domains. Neuron 22, 525–536.
Tian, L., Duncan, R.R., Hammond, M.S., Coghill, L.S., Wen, H., Rusinova, R., Clark, A.G., Levitan, I.B., Shipston, M.J., 2001. Alternative splicing switches potassium channel sensitivity to protein phosphorylation. J. Biol. Chem. 276, 7717–7720.
Tierney, A.J., Harris-Warrick, R.M., 1992. Physiological role of the transient potassium current in the pyloric circuit of the lobster stomatogastric ganglion. J. Neurophysiol. 67, 599–609.

Tsunoda, S., Salkoff, L., 1995. Genetic analysis of *Drosophila* neurons: Shal, Shaw, and Shab encode most embryonic potassium currents. J. Neurosci. 15, 1741–1754.

Yang, E.K., Alvira, M.R., Levitan, E.S., Takimoto, K., 2001. Kv beta subunits increase expression of Kv4.3 channels by interacting with their C-termini. J. Biol. Chem. 276, 4839–4844.

Wei, A., Covarrubias, M., Butler, A., Baker, K., Pak, M., Salkoff, L., 1990. K+ current diversity is produced by an extended gene family conserved in *Drosophila* and mouse. Science 248, 599–603.

(*Accepted* 15 *June* 2001)